Published in final edited form as:

Cancer Res. 2015 January 15; 75(2): 367–377. doi:10.1158/0008-5472.CAN-14-2304.

miR30a Inhibits LOX Expression and Anaplastic Thyroid Cancer Progression

Myriem Boufraqech[1], **Naris Nilubol**[1], **Lisa Zhang**[1], **Sudheer Kumar Gara**[1], **Samira M. Sadowski**[1], **Amit Mehta**[1,2], **Mei He**[1], **Sean Davis**[3], **Jennifer Dreiling**[4], **John A. Copland**[5], **Robert C. Smallridge**[5,6], **Martha M. Quezado**[4], **Electron Kebebew**[1]

[1]Endocrine Oncology Branch, Center for Cancer Research, NCI, NIH, Bethesda, Maryland. [2]Geisel School of Medicine at Dartmouth, Hanover, New Hampshire. [3]Genetics Branch, Center for Cancer Research, National Cancer Institute, NIH, Bethesda, Maryland. [4]Laboratory of Pathology, Center for Cancer Research, NCI, NIH, Bethesda, Maryland. [5]Department of Cancer Biology, Mayo Clinic, Jacksonville, Florida. [6]Endocrinology Division, Internal Medicine Department, Mayo Clinic, Jacksonville, Florida.

Abstract

Anaplastic thyroid cancer (ATC) is one of the most lethal human malignancies, but its genetic drivers remain little understood. In this study, we report losses in expression of the miRNA miR30a, which is downregulated in ATC compared with differentiated thyroid cancer and normal tissue. miR30a downregulation was associated with advanced differentiated thyroid cancer and higher mortality. Mechanistically, we found miR30a decreased cellular invasion and migration, epithelial-mesenchymal transition marker levels, lysyl oxidase (LOX) expression, and metastatic capacity. LOX was identified as a direct target of miR30a that was overexpressed in ATC and associated with advanced differentiated thyroid cancer and higher mortality rate. Consistent with its role in other cancers, we found that LOX inhibited cell proliferation, cellular invasion, and migration and metastasis *in vitro* and *in vivo*. Together,our findings establish a critical functional role for miR30a downregulation in mediating LOX upregulation and thyroid cancer progression, with implications for LOX targeting as a rational therapeutic strategy in ATC.

Corresponding Author: Electron Kebebew, National Cancer Institute, Room 45952, 10 Center Drive, MSC 1201, Bethesda, MD 20892-1201. Phone: 301-496-5049; Fax: 301-402-1788; kebebewe@mail.nih.gov.

Authors' Contributions

Conception and design: E. Kebebew, M. Boufraqech

Development of methodology: E. Kebebew, M. Boufraqech, N. Nilubol, L. Zhang, J.A. Copland

Acquisition of data (provided animals, acquired and managed patients, provided facilities, etc.): E. Kebebew, M. He, J. Dreiling, R.C. Smallridge, M.M. Quezado

Analysis and interpretation of data (e.g., statistical analysis, biostatistics, computational analysis): E. Kebebew, M. Boufraqech, N. Nilubol, S.M. Sadowski, A. Mehta, S. Davis

Writing, review, and/or revision of the manuscript: E. Kebebew, M. Boufraqech, N. Nilubol, L. Zhang, S.K. Gara, A. Mehta, S. Davis, J.A. Copland, R.C. Smallridge, M.M. Quezado

Administrative, technical, or material support (i.e., reporting or organizing data, constructing databases): N. Nilubol, S. Davis

Study supervision: E. Kebebew

Supplementary data for this article are available at Cancer Research Online (http://cancerres.aacrjoumals.org/).

Disclosure of Potential Conflicts of Interest

No potential conflicts of interest were disclosed.

Introduction

Anaplastic thyroid cancer (ATC) is one of the most lethal human malignancies, and is associated with a median survival of less than 6 months after diagnosis (1, 2). Over two-thirds of patients with ATC present with locally advanced and metastatic disease (2, 3). A number of different treatment modalities, including external beam radiotherapy, chemotherapy, and more recently, tyrosine kinase inhibitors, have been used, but have had limited efficacy (3–5). ATC represents one of the most aggressive human malignancies and the molecular events that are involved in ATC initiation and progression are poorly understood. Understanding the genetic changes involved in ATC initiation and progression may help in the development of more effective therapy for ATC and other aggressive solid malignancies.

It is now evident that, in addition to alterations in protein-coding genes, abnormalities in non-protein-coding genes can also contribute to cancer initiation and progression. miRNAs, by targeting the 3'UTR region of mRNAs, have been shown to silence target genes and thus can have important regulatory roles in a variety of cellular processes. Moreover, recent evidence indicates that some miRNAs can function either as oncogenes or tumor suppressor genes (6). However, the role of miRNA in ATC initiation and progression has not been completely investigated. ATC is characterized by loss of differentiation and is thought to originate from differentiated thyroid cancer of follicular cell origin (7). miRNAs have been shown to be involved in cellular differentiation (8, 9). Thus, analysis of the miRNA profile in ATC could provide new information on the molecular mechanisms involved in thyroid cancer progression.

In this study, we performed miRNA expression profiling in ATC, differentiated thyroid cancer, and normal thyroid tissues and found miR30a to be downregulated in ATC. We validated these data using The Cancer Genome Atlas (TCGA) data and found that miR30a downregulation was associated with more aggressive thyroid cancer histologies, advanced differentiated thyroid cancer, and higher mortality rate. We performed in vitro and in vivo functional studies in ATC cells, demonstrating that miR30a regulated cellular invasion, migration, and metastasis. Lysyl oxidase (LOX) was identified as a direct target of miR30a, and its expression levels was inversely correlated in thyroid cancer tissue samples. Functional studies with direct knockdown of LOX and inhibition of LOX activity recapitulated the effects of miR30a *in vitro* and *in vivo*. On the basis of these findings, we propose that there is a miR30a–LOX axis that regulates thyroid cancer progression, and that it could serve as an important therapeutic target for ATC.

Materials and Methods

Tissue samples and patient information

Thyroid tissue was obtained at the time of surgical resection, snap-frozen, and stored at −80°C. Serial tissue sample sections were used for RNA extraction, stained with hematoxylin and eosin, and reviewed by a pathologist to confirm the diagnosis and to ensure tumor nuclei content of >80%. The study was approved by the Office for Human Research Protections, at the Department of Health and Human Services. Patient information was

collected prospectively under an Institutional Review Board-approved protocol at the NIH (Bethesda, MD) after obtaining written informed consent.

miRNA profiling array

Twenty RNA samples [6 normal thyroid samples, 6 papillary thyroid cancer (PTC), and 8 anaplastic thyroid cancer (ATC)] were labeled using miRCURY LNA microRNA Hi-Power Labeling Kit (Exiqon). The labeled samples were hybridized to the miRCURY LNA microRNA Arrays. The dataset from Exiqon was loaded into Partek Genomics Suite (v6.6; Partek Inc.). To perform quality control and statistical analysis, one-way ANOVA was applied in the analysis with two linear contrasts. One contrast was to compare ATC to normal and another contrast was to compare ATC with PTC. The fold change was set at > ±1.5, false discovery rate (adjusted *P* value) <0.05. Differential expression (DE) of miRNAs between ATC and normal was 64 and DE miRNAs between ATC and PTC was 93. The intersection of DE miRNAs was 31. The 31 differentially expressed miRNAs are shown in Fig. 1A by Hierarchical Clustering.

Cell culture and reagents

The 8505C cell line was purchased from the European Collection of Cell Cultures. The human anaplastic thyroid cancer cell lines THJ-11T and THJ-16T were obtained from Dr. Copland (Mayo Clinic, Jacksonville, FL). The SW1736 cell line was purchased from Cell Lines Service (CLS). The ATC cell lines were maintained in DMEM with 4,500 mg/L D-glucose, 2 mmol/L L-glutamine, and 110 mg/L sodium pyruvate, supplemented with 10% FBS, penicillin (10,000 U/mL), streptomycin (10,000 U/mL), and fungizone (250 mg/mL), in a standard humidified incubator at 37°C, in a 5% CO_2 atmosphere. All cell lines were authenticated using short tandem repeat profiling.

For the LOX inhibition study, the cells were treated for 48 hours with 0 to 300 μmol/L β-aminopropionitrile (BAPN, Sigma Aldrich).

Cell transfection

A miR30a mimic, and its corresponding negative control miRNAs (miR-C; *mir*Vana miRNA mimic, Applied Biosystems), siLOX and siControl (siC; Applied Biosystems), were transiently transfected into 2×10^5 cells in 6-well plates using the transfection reagent RNAiMax (Life Technologies, Invitrogen), according to the manufacturer's protocol.

ATC cells were seeded into a 96-well plate (15,000 cells/well). After 24 hours, the cells were cotransfected with a GoClone reporter vector containing the 3'UTR region of LOX (SwitchGear Genomics) and the miR30a mimic (Applied Biosystems), using the Lipofectamine 2000 reagent (Invitrogen) according to the manufacturer's protocol. Luciferase activity was measured 24 hours after transfection using the LightSwitch Luciferase Assay reagent (SwitchGear Genomics) according to the manufacturer's protocol.

RNA extraction

Total RNA was extracted from snap-frozen tissues and cell lines using TRIzol reagent (Invitrogen) according to the manufacturer's protocol. RNA yield was determined using a NanoDrop 2000 spectrophotometer (Thermo Scientific).

Real-time RT-PCR

miRNA and gene expression levels were measured using specific primers and probes. Briefly, for miRNA detection, 5 ng of total RNA were reverse transcribed using a miRNA Reverse Transcription Kit (cat no. 4366597; Applied Biosystems), followed by amplification using an ABI 7500 RT-PCR system (Applied Biosystems). U6 snRNA was used as an endogenous control as we observed no significant variation in its expression by histologic subtype of thyroid cancer and under different transfection conditions. For gene expression, 500–1,000 ng of total RNA were reverse transcribed using a High Capacity Reverse Transcription cDNA kit (cat no. 4374967; Applied Biosystems), and the resulting cDNA was diluted and amplified according to the manufacturer's instructions. *GAPDH* was used as an endogenous control as we observed no significant variation in its expression by histologic subtype of thyroid cancer and under different transfection conditions. miRNA and gene expression levels were calculated using SDS 2.3 software (Applied Biosystems).

Cell invasion and migration assay

Cell invasion and migration were assessed using a Transwell chamber assay (BD Biosciences) according to the manufacturer's protocol, with and without Matrigel, respectively. The lower chamber of the plate was filled with 750 μL DMEM supplemented with 10% FBS as a chemoattractant. After 22 hours of incubation at 37°C, the cells invading through the bottom surface of the inserts were fixed, stained with Diff-Quik (Dade Behring), and photographed and counted using Image J software (NIH, Bethesda, MD).

Immunohistochemistry

Sections were deparaffinized and rehydrated, and antigen retrieval was performed with citrate buffer in a water bath at 120°C. The sections were incubated with the anti-LOX antibody (1:100, Abcam) overnight at 4°C, followed by incubation with a biotinylated secondary antibody for 1 hour at room temperature. The slides were developed with DAB [Dako EnVision+ system HRP (DAB), Dako] and counterstained with hematoxylin. The slides were scanned at ×20 magnification using a ScanScope XT digital slide scanner (Aperio Technologies, Inc.) to create whole-slide image data files at 0.5 μm/pixel resolution and viewed using ImageScope software (Aperio Technologies).

Tissue microarrays were purchased from US Biomax (#TH641). This array included duplicates of six follicular adenomas, six follicular thyroid carcinomas, six papillary thyroid carcinomas, six anaplastic thyroid carcinomas, and 16 normal tissues from lungs, thyroid, and testis.

Apoptosis assay

Caspase-Glo 3/7 substrate (Promega) was added to 30,000 transfected cells and incubated for 30 minutes at room temperature. Caspase activity was measured in each sample using a SpectraMax microplate reader (Molecular Devices).

Cell death assessment

Cells were assessed for viability with a fluorescence-based calcein–ethidium homodimer assay (10). Intracellular esterase activity in viable cells induces cell-permeate calcein-AM to fluoresce green, whereas ethidium homodimer crosses the permeable membranes of nonviable cells and fluoresces red.

Cell proliferation and clonogenic assays

For the cell proliferation assay, 1,500 ATC cells were seeded and transfected in a 96-well plate. The CyQUANT Cell Proliferation Assay kit (Invitrogen) was used to evaluate cell growth, according to the manufacturer's instruction. For the clonogenic assay, 1,000 ATC cells transfected with miR30a, miR-Control (miR-C), siControl, or siLOX were seeded in 6-well plates. After 10 days, the cells were washed with PBS and stained with 0.5% crystal violet.

Western blot analysis

Total protein lysates were subjected to SDS-PAGE, transferred to nitrocellulose membranes, and immunostained with the following antibodies overnight at 4° C: anti-vimentin (1:1,000, Abcam); anti-CD44 (1:1,000, Cell Signaling Technology), anti-N-cadherin (1:1,000, Millipore); anti-GAPDH (1:5,000, Santa Cruz Biotechnology). Anti-human GAPDH (1:5,000, Santa Cruz Biotechnology) was used as a loading control. Membranes were incubated with appropriate horseradish peroxidase-conjugated IgG (anti-rabbit 1:3,000, Cell Signaling Technology, or anti-mouse 1:10,000, Santa Cruz Biotechnology), and proteins were detected using enhanced chemiluminescence (ECL, Pierce Biotechnology).

Luciferase Assay

Cells were seeded in triplicate into a 96-well plate and cultured for 24 hours. The pLightSwitch 3'UTR reporter gene plasmids (pLightSwitch-LOX-3'UTR or pLightSwitch-Empty-3'UTR) were cotransfected with miR-C mimic or miR30a mimic (*miRVana*; Applied Biosystems) into the cells using Lipofectamine 2000 reagent (Invitrogen). Luciferase activity was measured 24 hours after transfection using the LightSwitch Luciferase Assay System (Switchgear Genomics), following the manufacturer's instructions.

Metastasis mouse model and drug administration

The animal studies were approved by the NCI's Institutional Animal Care and Use Committee. Five-week-old female athymic NCr-nu/nu mice were obtained from the Frederick Cancer Center Animal Facility (Frederick National Laboratory for Cancer Research, Frederick, MD). The mice were maintained according to guidelines set forth by NCI's Animal Research Advisory Committee. For the metastasis model, 30,000 8505C-Luc cells transfected with miR30a or siLOX or their corresponding controls, miR-C mimic or

siControl, were injected into the tail veins of Cg-*Prkdc*^{scid} *Il2rg*^{tm1Wjl}/SzJ mice (11). The mice were injected intraperitoneally with 30 mg/mL of luciferin. After anesthesia, the mice were imaged, and the images were analyzed using IVIS Living Image software (Caliper Life Sciences Inc).

For the drug treatment, the mice were randomly assigned to different treatment groups. Treatment with BAPN (Sigma Aldrich) at a dose of 100 mg/kg in 100 μL PBS was initiated either 24 hours before (group BAPN −1) or after (group BAPN +1) the cells were injected into the tail veins. BAPN injections were performed daily (day 1: intraperitoneally, day 2: intravenously) until the end of the experiment. A control group of mice received daily injections with vehicle (PBS) only.

Correlative analyses

Two publicly available genomic datasets were used. The GSE33630 dataset with 105 thyroid samples was downloaded from the National Center for Biotechnology Information Gene Expression Omnibus (12). This data was generated using 11 anaplastic thyroid carcinomas (ATC), 49 papillary thyroid carcinomas (PTC), and 45 normal thyroids (N) using Affymetrix U133 Plus 2.0 arrays. The normalized intensity values for LOX (probeset ID 204298_s_at and 215446_s_at) were extracted for analysis using all of the samples. The second dataset was downloaded from the NCI's TCGA data portal (13). Normalized intensity values (log 10) for LOX and miR30a were obtained from 454 PTC samples.

Statistical analyses

Statistical analyses were performed using GraphPad Prism 5 software (GraphPad Software). Parametric and nonparametric data were analyzed using a two-tailed *t* test and the Mann–Whitney *U* test, respectively. A value of $P < 0.05$ was considered statistically significant. Data are presented as mean ± SD or mean ± SEM.

Results

miR30a is downregulated in ATC and is associated with more aggressive histologic variants, advanced differentiated thyroid cancer, and higher mortality

We analyzed miRNA expression profiles in 8 ATC, 6 PTC, and 6 normal thyroid samples. Among the 31 significantly downregulated miRNAs in ATC, we found miR30a to be one of the most dysregulated miRNAs (ATC vs. N; adjusted $P = 0.013$; fold change = −3.25, ATC vs. PTC; adjusted $P = 0.012$; fold change = −3.26; Fig. 1A). We validated the expression level of miR30a by quantitative RT-PCR in 17 normal, 21 PTC, 6 poorly differentiated thyroid cancer (PDTC), and 10 ATC samples and found that miR30a was significantly downregulated in ATC and PDTC compared with PTC and normal thyroid samples (Fig. 1B). To determine whether there is an association between miR30a expression level and clinicopathologic characteristics of patients with thyroid cancer, we used the NCI's TCGA thyroid cancer database. miR30a expression levels were significantly lower in advanced thyroid cancer (Fig. 1C). Furthermore, patients with thyroid cancer with tumors that had lower miR30a expression had a higher mortality rate (Fig. 1D).

miR30a overexpression inhibits cellular invasion and migration, and decreases cell proliferation *in vitro*

Given the significant reduction in miR30a expression in ATC and PDTC and its association with aggressive disease in differentiated thyroid cancer (i.e., PTC), we next asked whether miR30a regulated the hallmarks of cancer progression: cellular invasion and migration, epithelial-to-mesenchymal transition (EMT), and proliferation. We used miR30a overexpression and inhibition strategies in ATC cell lines (8505C, THJ-11T, THJ-16T, and SW1736; Supplementary Fig. S1A and S1B). Cell proliferation and clonogenic assays demonstrated that overexpression of miR30a leads to a significant decrease in cell proliferation and colonies (Fig. 2A). To determine the mechanism by which miR30a regulates cell proliferation, apoptosis assays were performed. Cells were stained with calcein-AM and ethidium homodimer-1 to show the ratio of live cells (green: calcein-AM stained) to apoptotic or dead cells (red: ethidium bromide homodimer-1 stained). Overexpression of miR30a increased cell death (Fig. 2B). To determine whether miR30a-induced apoptosis was caspase-dependent, caspase activity assays were performed. Caspase-3/7 activity was significantly higher in cells overexpressing miR30a compared with miR-C (Fig. 2C).

Given that cell migration is among the common functions required by tumor cells for metastatic progression, we asked whether increased miR30a expression could modulate the invasive capacity of ATC cells. We found cellular invasion and migration were significantly reduced with miR30a overexpression compared with miR-C–transfected cells (Fig. 2D and Supplementary Fig. S2A). Because EMT increases the metastatic ability of cancer cells, we investigated the effect of miR30a on EMT marker expression. To determine whether miR30a alters EMT markers, we used Western blot analysis to examine the expression levels of two EMT markers: vimentin and N-cadherin. The reduced cellular invasion and migration caused by miR30a overexpression was accompanied by decreased expression of N-cadherin and vimentin. Increased expression of the stem cell marker CD44 has been associated with cellular invasion, migration, and metastasis. We found decreased CD44 expression in ATC cells overexpressing miR30a (Fig. 2E).

miR30a inhibits metastasis *in vivo*

In view of the fact that our in vitro experiments showed that miR30a overexpression inhibited prometastatic traits in ATC cells, we investigated whether miR30a plays a role in tumor suppression using our *in vivo* mouse model of thyroid cancer metastasis (11). 8505C-Luc-miR30a cells and their corresponding control miR-C cells were injected into the tail veins of Cg-*Prkdc*^{scid} *Il2rg*^{tm1Wjl}/SzJ mice. Mice bearing 8505C-Luc-miR-C tumors displayed prominent lung metastases, whereas smaller metastases were found in the mice injected with 8505C-Luc-miR30a cells (Fig. 2F, right). Next, we tested whether miR30a could play a role in tumor growth by using a nude mouse flank xenograft model. Overexpression of miR30a in 8505C-Luc cells did not affect tumor growth in nude mice (Fig. 2F, left). Taken together, the miR30a expression data from human thyroid cancer samples and the *in vitro* and *in vivo* data showing that miR30a overexpression inhibits cellular invasion and migration, and metastasis, but not *in vivo* cellular growth, suggest that miR30a is involved in thyroid cancer progression.

LOX is a direct target of miR30a

Having identified miR30a as a suppressor of thyroid cancer progression, we became interested in identifying which gene(s) this miRNA might regulate in ATC. As miR30a was downregulated in ATC and PDTC samples, we reasoned that its potential direct targets would be upregulated. Therefore, we analyzed genes from the publicly available GSE33630 dataset that are upregulated in ATC. These potential miR30a target genes were obtained using the miRDB and TargetScan prediction algorithms. We found *LOX* to be a gene of special interest among other genes regulated by miR30a (and highly expressed only in ATC) because it has been recently associated with metastasis and lower survival rates in aggressive breast cancer (14, 15). However, the mechanism leading to upregulation of LOX in metastatic cancers is unknown.

Overexpression of miR30a in ATC cells decreased LOX protein expression in four ATC cell lines with low basal miR30a expression levels (Fig. 3A). To determine whether LOX is regulated by miR30a through direct binding to the 3'UTR region of *LOX*, the LOX- 3'UTR was inserted into a luciferase reporter vector. Transfection of 3'UTR-LOX, along with miR30a, into ATC cell lines led to a significant decrease in luciferase activity compared with the cotransfection of 3'UTR-*LOX* with miR-C (Fig. 3B).

LOX is upregulated in aggressive thyroid cancer

To determine the expression pattern of LOX in thyroid cancer, we analyzed LOX expression by RT-PCR in normal, PTC, PDTC, and ATC tissues. We found that ATC tissues had significantly higher LOX expression than differentiated thyroid cancer and normal thyroid tissues (Fig. 4A). Furthermore, analysis of the LOX expression profile in different histologic subtypes of thyroid cancer using data from TCGA showed significantly higher LOX expression in the aggressive tall cell variant of PTC (TC-PTC) compared with the differentiated thyroid cancers [classic PTC (cPTC) and follicular variant of PTC (FV-PTC); Fig. 4B]. We also found that high LOX expression in tumors was associated with extrathyroidal invasion and a higher mortality rate (Fig. 4C and D).

We next evaluated the correlation between miR30a and *LOX* mRNA expression in our sample set. The expression levels of miR30a and *LOX* showed an inverse correlation ($r = -0.59$, $P < 0.0001$; Fig. 4E). Similarly, there was a significant inverse correlation between miR30a and *LOX* in 454 thyroid cancer samples from TCGA ($r = -0.54$, $P < 0.0001$; Fig. 4F). These results are consistent with *in vitro* studies showing that miR30a directly targets *LOX*. We also performed immunohistochemical analysis of LOX protein expression in eight TC-PTC and six cPTC samples, and in an independent tissue microarray that included thyroid cancer, benign thyroid neoplasm, and normal thyroid tissue, and observed high expression of LOX protein in aggressive thyroid cancer histologic variants (i.e., TC-PTC) and ATC samples, but not in normal, benign, and differentiated thyroid cancer samples (Fig. 4G and H).

LOX inhibition decreases anaplastic thyroid cancer invasion and metastasis

To determine whether *LOX* recapitulates the effects of miR30a observed in ATC cells, ATC cell lines were treated with BAPN, an irreversible inhibitor of the amine oxidase activity of

LOX (16, 17). Treatment of ATC cells with BAPN did not affect cellular proliferation, but did inhibit cellular invasion and migration in three of four cell lines (Fig. 5A and B and Supplementary Fig. S2B). BAPN treatment also decreased expression of the EMT marker vimentin in all ATC cell lines; however, no difference in N-cadherin expression was observed (Fig. 5C). We next investigated whether *LOX* had a significant role in metastasis. To evaluate the effect of LOX activity inhibition on the development of metastases, we randomly assigned mice into two experimental groups (four mice/group) that received daily injections of BAPN or PBS, starting 24 hours before and after tail-vein injection of 8505c-Luc-positive cells. Analysis of tumor burden in the mice over time revealed that BAPN significantly reduced development of metastases (Supplementary Fig. S3A). As BAPN can inhibit the amine oxidase of LOX-like proteins also, siRNA targeting only *LOX* were used *in vivo* and *in vitro*. RT-PCR, Western blot analysis, and immunofluorescence assays showed that LOX expression was significantly lower in siLOX-transfected cells than in control cells (Fig. 6A). Cell proliferation and clonogenic assays showed that knockdown of LOX expression significantly reduced cell growth and colonies (Fig. 6B) and increased caspase activity (Fig. 6C). Finally, knockdown of LOX expression also decreased ATC cellular invasion and migration (Fig. 6D and Supplementary Fig. 3B).

To determine the role of LOX in ATC cell metastasis in vivo, transiently transfected 8505c-Luc cells were injected, with siLOX or siControl, into the tail veins of Cg-*Prkdc*^{scid} *Il2rg*^{tm1Wjl}/SzJ mice. Analysis of the tumor burden over time showed that LOX knockdown significantly inhibited metastasis to the lung (Fig. 6E and F). To further validate *LOX* as a target of miR30a, LOX expression in lung metastases from miR-C and miR30a mice was also analyzed. Immunostaining for LOX showed lower levels of LOX in miR30a mice compared with miR-C mice. Lower LOX levels were also accompanied by decreased N-cadherin and vimentin expression in the metastatic tumors from the miR30a mice compared with miR-C mice (Fig. 6G). Taken together, the findings of our functional *LOX* studies are consistent with the effects observed for miR30a expression in ATC cells, suggesting that a miR30-LOX axis plays a role in regulating thyroid cancer progression.

Discussion

In this study, we demonstrated a key role for miR30a in thyroid cancer progression. Analysis of miR30a expression in thyroid cancer showed downregulation of miR30a in PDTC and ATC, and an association between lower miR30a expression levels in advanced thyroid cancer and higher mortality rates in differentiated thyroid cancer. Overexpression of miR30a decreased cellular invasion and metastasis, and inhibited the expression of two EMT markers and the stem cell marker CD44, which are all associated with cancer progression (18, 19). These observations led us to investigate the mechanism of action of miR30a in ATC, finding that it directly targets *LOX*, which recapitulates the effect of miR30a on thyroid cancer progression based on its expression profile and our functional data.

miR30a is located on human chromosome 6q.13, which produces three miRNAs: miR30a, −30c, and −30e (20). miR30 family members are among one of the most dysregulated miRNAs in metastatic cancers, each with a potential role in cancer metastasis (21). Although miR30a expression has been reported to be downregulated in metastatic breast cancer and

colorectal cancer, its tumor suppressor function is not well understood (22, 23). Specifically, downregulation of miR30a in ATC has been previously reported but overexpression of this miRNA did not affect cell proliferation in two ATC cell lines (FRO, FB-1; ref. 24). In our study, we used 4 different ATC cell lines to confirm the role of miR30a in cell proliferation. It has been demonstrated that miR30 family regulate cellular invasion by targeting EMT-related genes such as SMAD2 in ATC cells, *Snail1* in non–small cell lung cancer cells or vimentin in breast cancer cells (25–27). Our study shows, for the first time, that miR30a has tumor-suppressive functions and is involved in cancer progression *in vitro* and *in vivo*, and that it directly targets *LOX* expression.

The LOX protein is a member of a five-member family of amine oxidases, which have been implicated in cancer progression (28). LOX is an extracellular matrix-remodeling enzyme and is required for the oxidative deamination of lysine residues in collagen and elastin molecules, a process that is responsible for fiber cross-linking in the extracellular matrix (ECM). In this process, LOX catalyzes the exchange of an amine to an aldehyde group on a peptidyl lysine, producing hydrogen peroxide and ammonia as by-products of its catalytic activity (28). Although ECM regulation has been considered the main function of LOX, recent studies have demonstrated that LOX is also involved in the regulation of cell differentiation, migration, and adhesion, as well as gene transcription (29–31). Upregulation of LOX expression and activity has been reported in various cancer tissues and tumor cell lines, and is associated with metastasis and poor prognosis (15, 32). Increased LOX has been associated with metastasis and decreased survival in patients with breast cancer, as well as patients with head and neck squamous cell carcinoma (14, 15).

Knockdown of LOX and inhibition of LOX activity in ATC cells significantly reduced cellular invasion, migration, and metastasis *in vitro* and *in vivo*. Furthermore, in a large thyroid cancer cohort, we found that high LOX expression is associated with extrathyroidal invasion and higher mortality. We also found an inverse correlation between miR30a and LOX expression in thyroid cancer samples. These data suggest that a miR30a-LOX axis is involved in thyroid cancer progression. Consistent with our data, patients with breast cancer with high LOX levels have been reported to have shorter survival times and a higher risk of metastasis (14, 33). Also, upregulation of LOX has been observed in colorectal carcinoma (34). Because colorectal carcinoma and breast cancer display downregulation of miR30a, a miR30a–LOX axis might be a dysregulated pathway not only in thyroid cancer progression, but also in other cancers.

Inhibition of LOX activity using BAPN failed to inhibit cell proliferation; however, knockdown of LOX using siRNA inhibited cell proliferation and increased caspase-dependent apoptosis. This suggests that the role of LOX in cell proliferation is not mediated by the catalytic activity of LOX. These findings may be of importance to current investigations into the development and evaluation of LOX-targeting agents for cancer therapy (35). This is the first study to show a role for LOX in cell proliferation and cell-cycle regulation. LOX is synthesized and secreted as an inactive, 50 kDa proenzyme, which is subsequently cleaved to yield a functional 32 kDa enzyme (LOX) and an 18 kDa propeptide. *In vivo* immunostaining of the 32 kDa LOX protein in ATC and TC-PTC tissue samples

showed strong staining in the nucleus. These data are consistent with results from a previous study showing that LOX regulates the transcriptional activity of TWIST-1 (33).

In conclusion, our study demonstrates, for the first time, the role of miR30a in suppressing ATC migration, invasion, and metastasis, likely mediated by LOX. miR30a expression inversely correlates with thyroid cancer aggressiveness and metastasis, supporting the hypothesis that lower miR30a levels lead to overexpression of LOX, which promotes thyroid cancer progression. Therefore, we propose that the miR30a–LOX axis could be targeted for ATC therapy.

Supplementary Material

Refer to Web version on PubMed Central for supplementary material.

Acknowledgments

The authors thank Dr. Jia Li for her help with analyzing some of the miRNA profiling data.

Grant Support

This research was supported by the intramural research program of the Center for Cancer Research, NCI, NIH.

The costs of publication of this article were defrayed in part by the payment of page charges. This article must therefore be hereby marked *advertisement* in accordance with 18 U.S.C. Section 1734 solely to indicate this fact.

References

1. Smallridge RC, Ain KB, Asa SL, Bible KC, Brierley JD, Burman KD, et al. American Thyroid Association guidelines for management of patients with anaplastic thyroid cancer. Thyroid 2012;22:1104–39. [PubMed: 23130564]
2. Kebebew E, Greenspan FS, Clark OH, Woeber KA, McMillan A. Anaplastic thyroid carcinoma. Treatment outcome and prognostic factors. Cancer 2005;103:1330–5. [PubMed: 15739211]
3. McIver B, Hayl D, Giuffrida DF, Dvorak CE, Grant CS, Thompson GB, et al. Anaplastic thyroid carcinoma: a 50-year experience at a single institution. Surgery 2001;130:1028–34. [PubMed: 11742333]
4. De Crevoisier R, Baudin E, Bachelot A, Leboulleux S, Travagli JP, Caillou B, et al. Combined treatment of anaplastic thyroid carcinoma with surgery, chemotherapy, and hyperfractionated accelerated external radiotherapy. Int J Radiat Oncol Biol Phys 2004;60:1137–43. [PubMed: 15519785]
5. Smallridge RC, Copland JA, Brose MS, Wadsworth JT, Houvras Y, Menefee ME, et al. Efatutazone, an oral PPAR-gamma agonist, in combination with paclitaxel in anaplastic thyroid cancer: results of a multicenter phase 1 trial. J Clin Endocrinol Metab 2013;98:2392–400. [PubMed: 23589525]
6. Bouyssou JM, Manier S, Huynh D, Issa S, Roccaro AM, Ghobrial IM. Regulation of microRNAs in cancer metastasis. Biochim Biophys Acta 2014;1845:255–65. [PubMed: 24569228]
7. Smallridge RC, Marlow LA, Copland JA. Anaplastic thyroid cancer: molecular pathogenesis and emerging therapies. Endocrine Relat Cancer 2009; 16:17–44.
8. Sempere LF, Freemantle S, Pitha-Rowe I, Moss E, Dmitrovsky E, Ambros V. Expression profiling of mammalian microRNAs uncovers a subset of brain-expressed microRNAs with possible roles in murine and human neuronal differentiation. Genome Biol 2004;5:R13. [PubMed: 15003116]
9. Chen CZ, Li L, Lodish HF, Bartel DP. MicroRNAs modulate hematopoietic lineage differentiation. Science 2004;303:83–6. [PubMed: 14657504]
10. Fortenberry JD, Owens ML, Brown MR, Atkinson D, Brown LA. Exogenous nitric oxide enhances neutrophil cell death and DNA fragmentation. Am J Resp Cell Mol Biol 1998;18:421–8.

11. Zhang L, Gaskins K, Yu Z, Xiong Y, Merino MJ, Kebebew E. An in vivo mouse model of metastatic human thyroid cancer. Thyroid 2014;24: 695–704. [PubMed: 24262022]
12. Barrett T, Wilhite SE, Ledoux P, Evangelista C, Kim IF, Tomashevsky M, et al. NCBI GEO: archive for functional genomics data sets-update. Nucleic Acids Res 2013;41:D991–5. [PubMed: 23193258]
13. Cancer Genome Atlas Research Network Weinstein JN, Collisson EA, Mills GB, Shaw KR, Ozenberger BA, et al. The Cancer Genome Atlas Pan-Cancer analysis project. Nat Genet 2013;45:1113–20. [PubMed: 24071849]
14. Erler JT, Bennewith KL, Nicolau M, Dornhofer N, Kong C, Le QT, et al. Lysyl oxidase is essential for hypoxia-induced metastasis. Nature 2006;440: 1222–6. [PubMed: 16642001]
15. Kirschmann DA, Seftor EA, Fong SF, Nieva DR, Sullivan CM, Edwards EM, et al. A molecular role for lysyl oxidase in breast cancer invasion. Cancer Res 2002;62:4478–83. [PubMed: 12154058]
16. Tang SS, Trackman PC, Kagan HM. Reaction of aortic lysyl oxidase with beta-aminopropionitrile. J Biol Chem 1983;258:4331–8. [PubMed: 6131892]
17. Bondareva A, Downey CM, Ayres F, Liu W, Boyd SK, Hallgrimsson B, et al. The lysyl oxidase inhibitor, beta-aminopropionitrile, diminishes the metastatic colonization potential of circulating breast cancer cells. PLoS ONE 2009;4:e5620.
18. Negi LM, Talegaonkar S, Jaggi M, Ahmad FJ, Iqbal Z, Khar RK. Role of CD44 in tumour progression and strategies for targeting. J Drug Target 2012; 20:561–73. [PubMed: 22758394]
19. Xia H, Hui KM. MicroRNAs involved in regulating epithelial-mesenchymal transition and cancer stem cells as molecular targets for cancer therapeutics. Cancer Gene Ther 2012;19:723–30. [PubMed: 22975591]
20. Rodriguez A, Griffiths-Jones S, Ashurst JL, Bradley A. Identification of mammalian microRNA host genes and transcription units. Genome Res 2004;14:1902–10. [PubMed: 15364901]
21. Baffa R, Fassan M, Volinia S, O'Hara B, Liu CG, Palazzo JP, et al. MicroRNA expression profiling of human metastatic cancers identifies cancer gene targets. J Pathol 2009;219:214–21. [PubMed: 19593777]
22. Zhang N, Wang X, Huo Q, Sun M, Cai C, Liu Z, et al. MicroRNA-30a suppresses breast tumor growth and metastasis by targeting metadherin. Oncogene 2013;33:3119–28. [PubMed: 23851509]
23. Zhong M, Bian Z, Wu Z. miR-30a suppresses cell migration and invasion through downregulation of PIK3CD in colorectal carcinoma. Cell Physiol Biochem 2013;31:209–18. [PubMed: 23486085]
24. Visone R, Pallante P, Vecchione A, Cirombella R, Ferracin M, Ferraro A, et al. Specific microRNAs are downregulated in human thyroid anaplastic carcinomas. Oncogene 2007;26:7590–5. [PubMed: 17563749]
25. Kumarswamy R, Mudduluru G, Ceppi P, Muppala S, Kozlowski M, Niklinski J, et al. MicroRNA-30a inhibits epithelial-to-mesenchymal transition by targeting Snai1 and is downregulated in non-small cell lung cancer. Int J Cancer 2012;130:2044–53. [PubMed: 21633953]
26. Cheng CW, Wang HW, Chang CW, Chu HW, Chen CY, Yu JC, et al. MicroRNA-30a inhibits cell migration and invasion by downregulating vimentin expression and is a potential prognostic marker in breast cancer. Breast Cancer Res Treat 2012;134:1081–93. [PubMed: 22476851]
27. Braun J, Hoang-Vu C, Dralle H, Huttelmaier S. Downregulation of microRNAs directs the EMT and invasive potential of anaplastic thyroid carcinomas. Oncogene 2010;29:4237–44. [PubMed: 20498632]
28. Mayorca-Guiliani A, Erler JT. The potential for targeting extracellular LOX proteins in human malignancy. Onco Targets Ther 2013;6:1729–35. [PubMed: 24348049]
29. Li W, Liu G, Chou IN, Kagan HM. Hydrogen peroxide-mediated, lysyl oxidase-dependent chemotaxis of vascular smooth muscle cells. J Cell Biochem 2000;78:550–7. [PubMed: 10861852]
30. Giampuzzi M, Oleggini R, Di Donato A. Altered adhesion features and signal transduction in NRK-49F cells transformed by down-regulation of lysyl oxidase. Biochim Biophys Acta 2003;1647:239–44. [PubMed: 12686140]
31. Alves CC, Carneiro F, Hoefler H, Becker KF. Role of the epithelial-mesenchymal transition regulator Slug in primary human cancers. Front Biosci 2009;14:3035–50.

32. Payne SL, Hendrix MJ, Kirschmann DA. Paradoxical roles for lysyl oxidases in cancer–a prospect. J Cell Biochem 2007;101:1338–54. [PubMed: 17471532]

33. El-Haibi CP, Bell GW, Zhang J, Collmann AY, Wood D, Scherber CM, et al. Critical role for lysyl oxidase in mesenchymal stem cell-driven breast cancer malignancy. Proc Natl Acad Sci U S A 2012;109:17460–5. [PubMed: 23033492]

34. Baker AM, Cox TR, Bird D, Lang G, Murray GI, Sun XF, et al. The role of lysyl oxidase in SRC-dependent proliferation and metastasis of colorectal cancer. J Natl Cancer Inst 2011;103:407–24. [PubMed: 21282564]

35. Barker HE, Cox TR, Erler JT. The rationale for targeting the LOX family in cancer. Nat Rev Cancer 2012;12:540–52. [PubMed: 22810810]

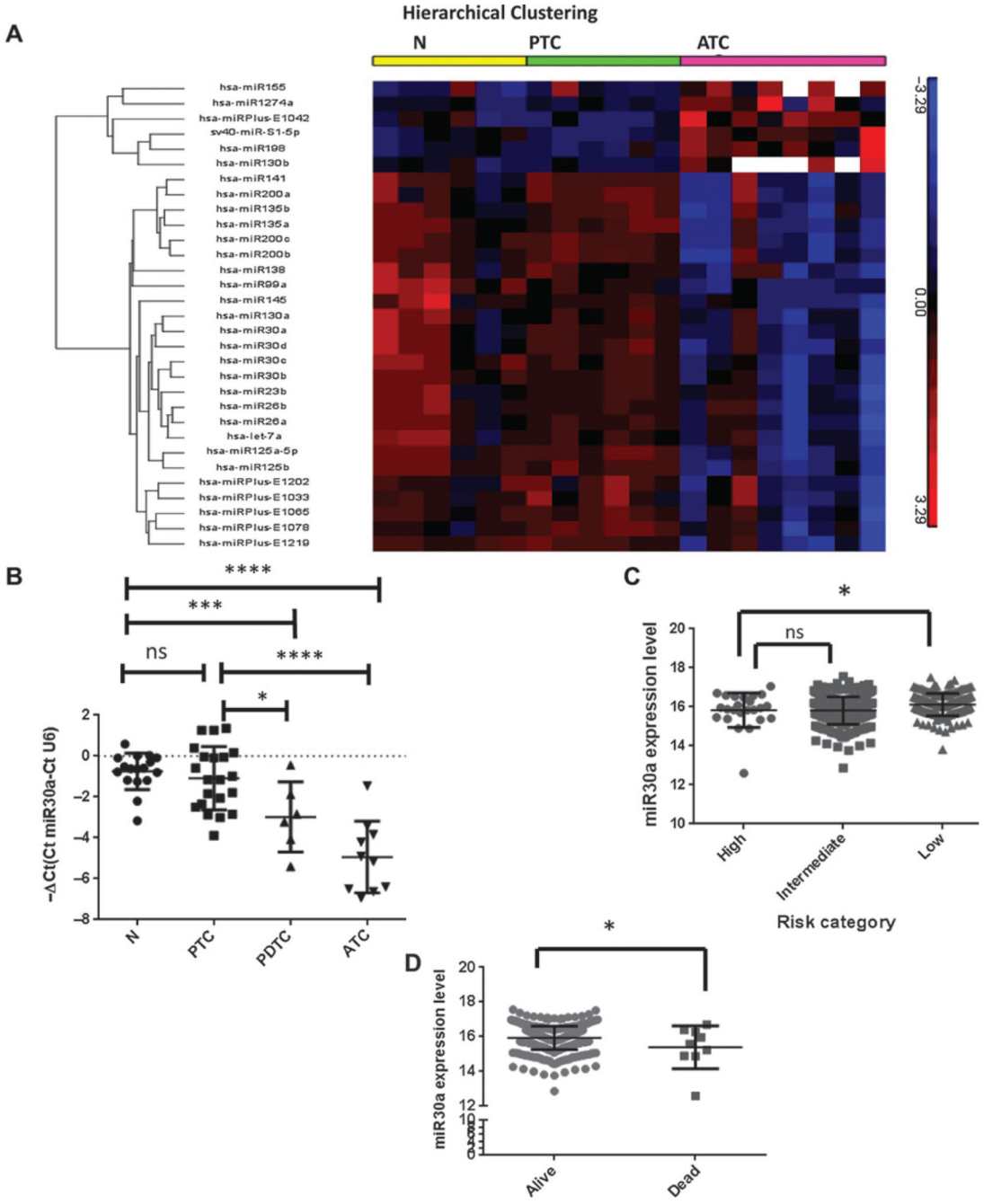

Figure 1.

miR30a expression in thyroid tissue. A, heatmap of differentially expressed miRNA in thyroid cancer samples. Supervised hierarchical clustering of miRNA expression in 20 tissue samples: 6 N, 6 PTC, and 8 ATC. Red, overexpression; green, underexpression. N, normal. B, miR30a expression is downregulated in the aggressive thyroid cancer PDTC:17N, 21 PTC, 10 ATC, and 6 PDTC samples were analyzed. *, $P < 0.05$; ***, $P < 0.001$; ****, $P < 0.0001$. C, miR30a expression by thyroid cancer risk group as defined by the MACIS prognostic scoring system. Data from NCI's TCGA program (accessed at

explorer.cancerregulome.org) showed significantly lower expression of miR30a in high-risk thyroid cancer, as defined by the MACIS risk group. *, $P < 0.05$; ns, not significant. D, miR30a expression is lower in patients who died from conventional PTC. *, $P < 0.05$.

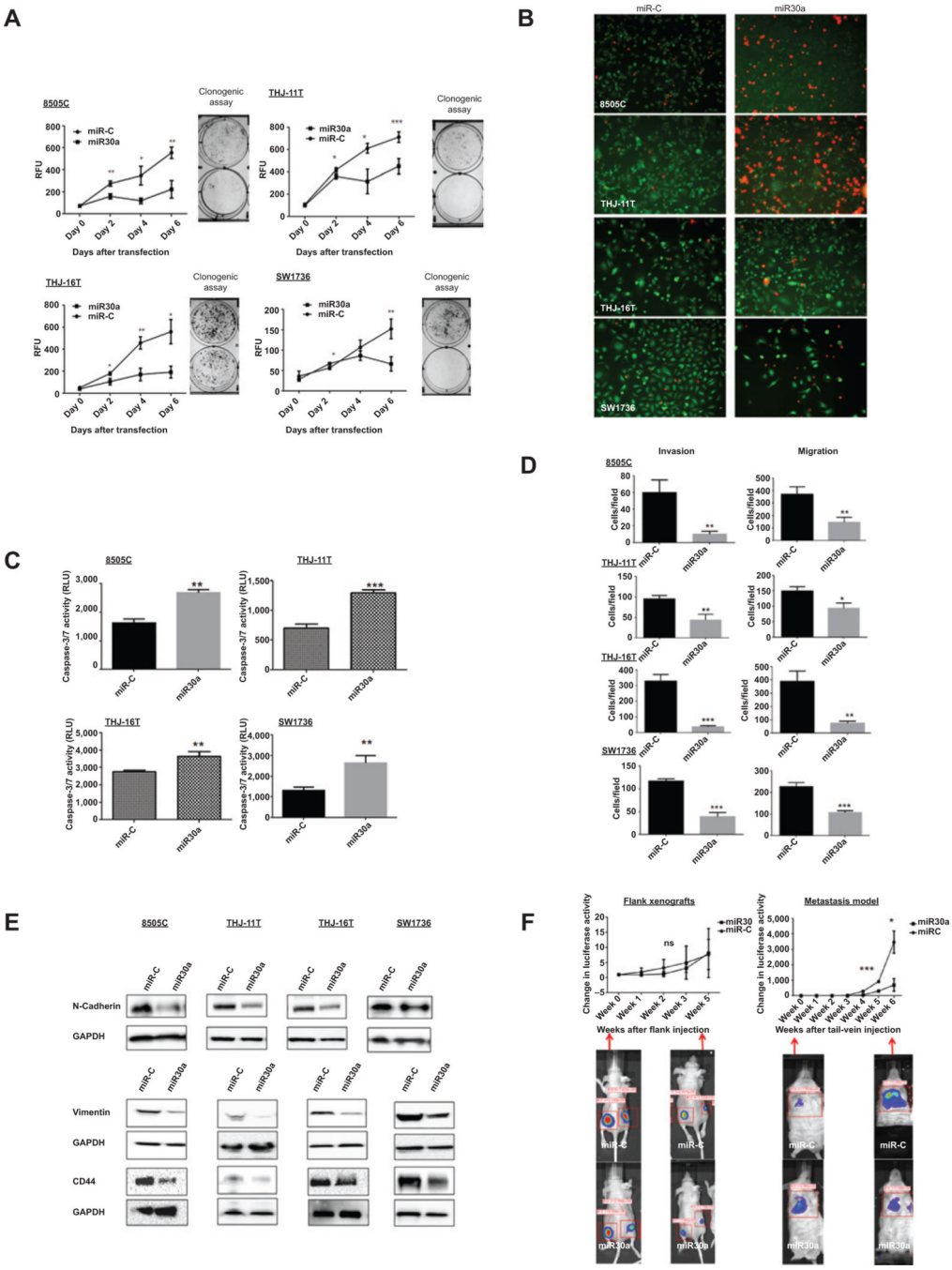

Figure 2.

Effect of miR30a on cellular proliferation, migration and invasion, apoptosis, and metastasis. A, miR30a inhibits cellular proliferation. The effect of miR30a overexpression was determined in four ATC cell lines, 8505C, THJ-11T, THJ-16T, and SW1736, using a CyQUANT Cell Proliferation Assay and a clonogenic assay after transfection with 25 nmol/L of miR30a or miR-C. miR30a transfection significantly inhibited cell proliferation and colonies formation compared with miR-C. *, $P < 0.05$; **, $P < 0.01$; ***, $P < 0.001$. B, representative images of ATC cells obtained using fluorescent microscopy. Viable cells

exhibit green fluorescence (calcein-AM), whereas membrane-permeable, nonviable cells exhibit red fluorescence (ethidium homodimer-1). Cells are shown 72 hours after transfection. C, ectopic expression of miR30a increased caspase-3/7 activity. Data shown are from 72 hours after transfection. **, $P < 0.01$; ***, $P < 0.001$. D, miR30a inhibits cellular migration and invasion. The Transwell assay showed that overexpression of miR30a markedly decreased invasion and migration in four ATC cell lines. These results are representative of at least three independent experiments. E, ectopic expression of miR30a reduces N-cadherin, vimentin, and CD44 expression compared with miR-C. F, effect of miR30a on tumor growth and metastasis *in vivo*. Nude mice were injected subcutaneously with 8505C-Luc cells expressing either miR-C or miR30a. Luciferase activity (mean±SD) was measured over time in flank xenograft (left) and metastatic (right) models. There was no significant difference in growth in the flank xenograft, but there was a significant difference in the number and volume of metastatic lesions in mice that had tail-vein injections of 8505C-Luc cells. Luciferase activity images of lung metastases in mice that received tail-vein injection of cells overexpressing miR30a (3 mice) or miR-C (3 mice). RFU, relative fluorescence unit. *, $P < 0.05$; **, $P < 0.01$; ***, $P < 0.001$.

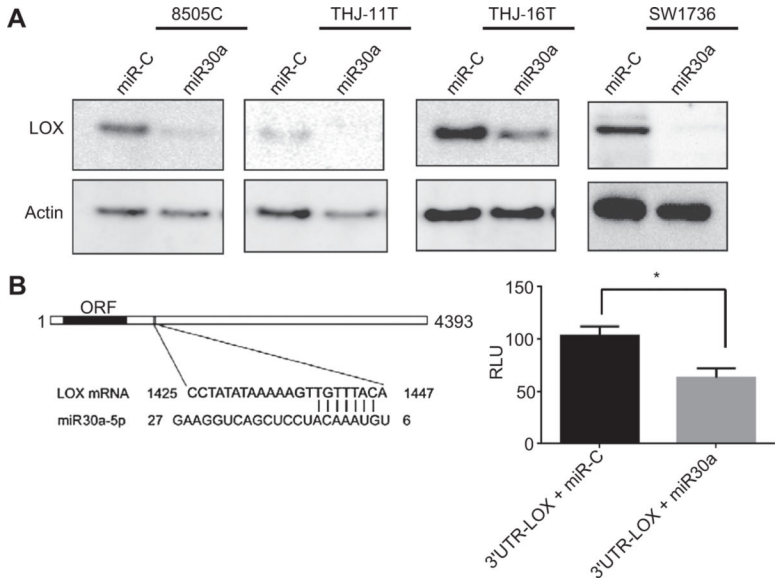

Figure 3.

Identification of *LOX* as a target gene of miR30a. A, miR30a regulates *LOX* expression. Western blot analysis shows reduced expression of LOX 72 hours after miR30a transfection. B, miR30a directly targets the 3'UTR of *LOX* mRNA. A luciferase vector was designed to include the region of the candidate target sequence for miR30a. Bar graph shows luciferase activity of the 3'UTR-LOX luciferase vector after cotransfection with miR-C or miR30a in THJ-16Tcells. *, $P < 0.05$.

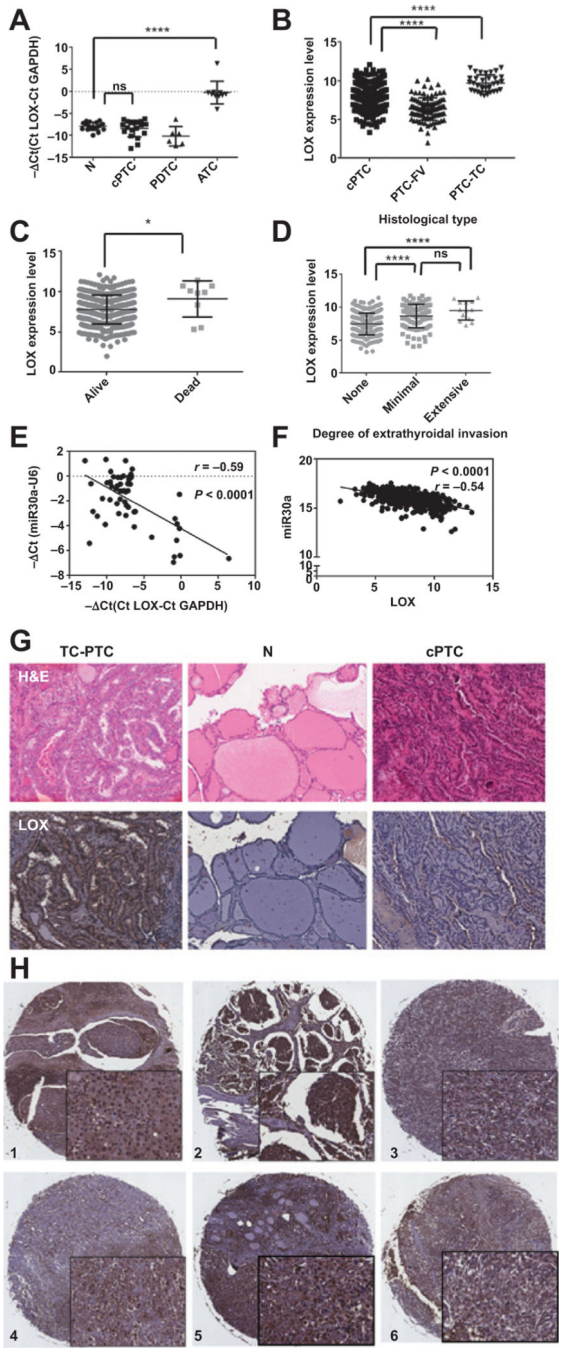

Figure 4.

Analysis of LOX expression in thyroid cancer samples. A, LOX expression, assayed by RT-PCR, is upregulated in our ATC cohort. B, validation of upregulated *LOX* expression in aggressive thyroid cancer in the thyroid cancer dataset from TCGA. C, *LOX* expression is higher in patients who die from thyroid cancer. D, high *LOX* expression in tumors is associated with local invasion. E and F, correlation between miR30a and *LOX* expression in our cohort (E) and the dataset from TCGA (F). G, representative LOX protein expression, as detected by immunohistochemistry, in TC-PTC, cPTC, and N thyroid tissue. LOX

expression is restricted to the tumor tissue, and its levels are higher in TC-PTC than in cPTC. N, normal. H, representative immunohistochemical staining of LOX protein in six ATCsamples. Magnification, ×6 and ×40. *, $P < 0.05$; **, $P < 0.01$; ***, $P < 0.001$; ****, $P < 0.0001$.

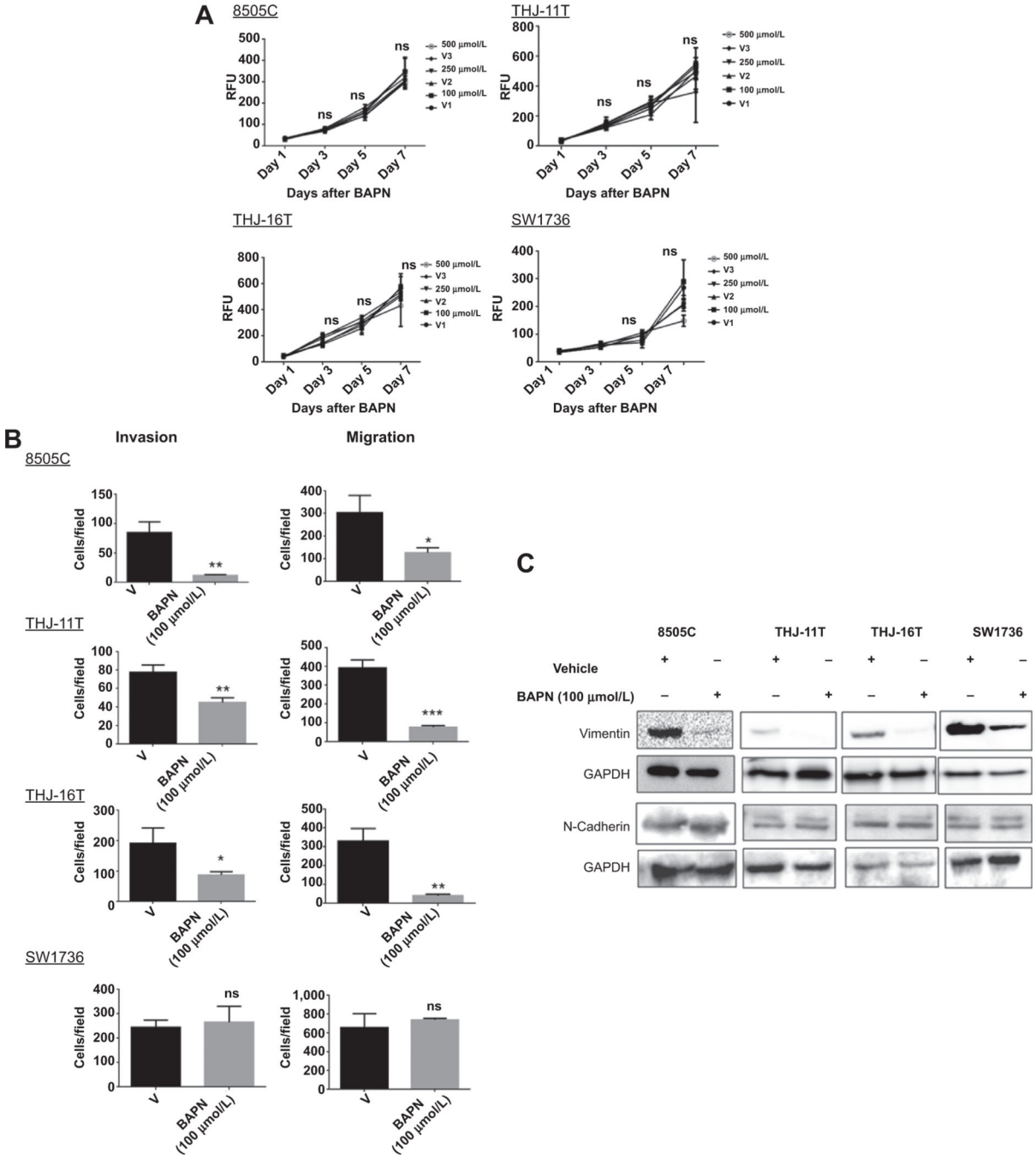

Figure 5.

Effect of LOX activity inhibition on thyroid cancer biology *in vitro* and *in vivo*. A, inhibition of LOX activity does not affect cellular proliferation. BAPN (100, 250, and 500 µmol/L) was used with a CyQUANT assay to evaluate the effect of LOX inhibition on cellular proliferation. B, LOX activity inhibition reduces cellular migration and invasion in ATC cell lines. Transwell migration and invasion assays were performed after 24 hours of treatment with and without 100 µmol/L of BAPN. C, LOX inhibition reduces only vimentin expression

in ATC cells. The cell lines were treated with and without 100 μmol/L of BAPN over 48 hours. RFU, relative fluorescence units.

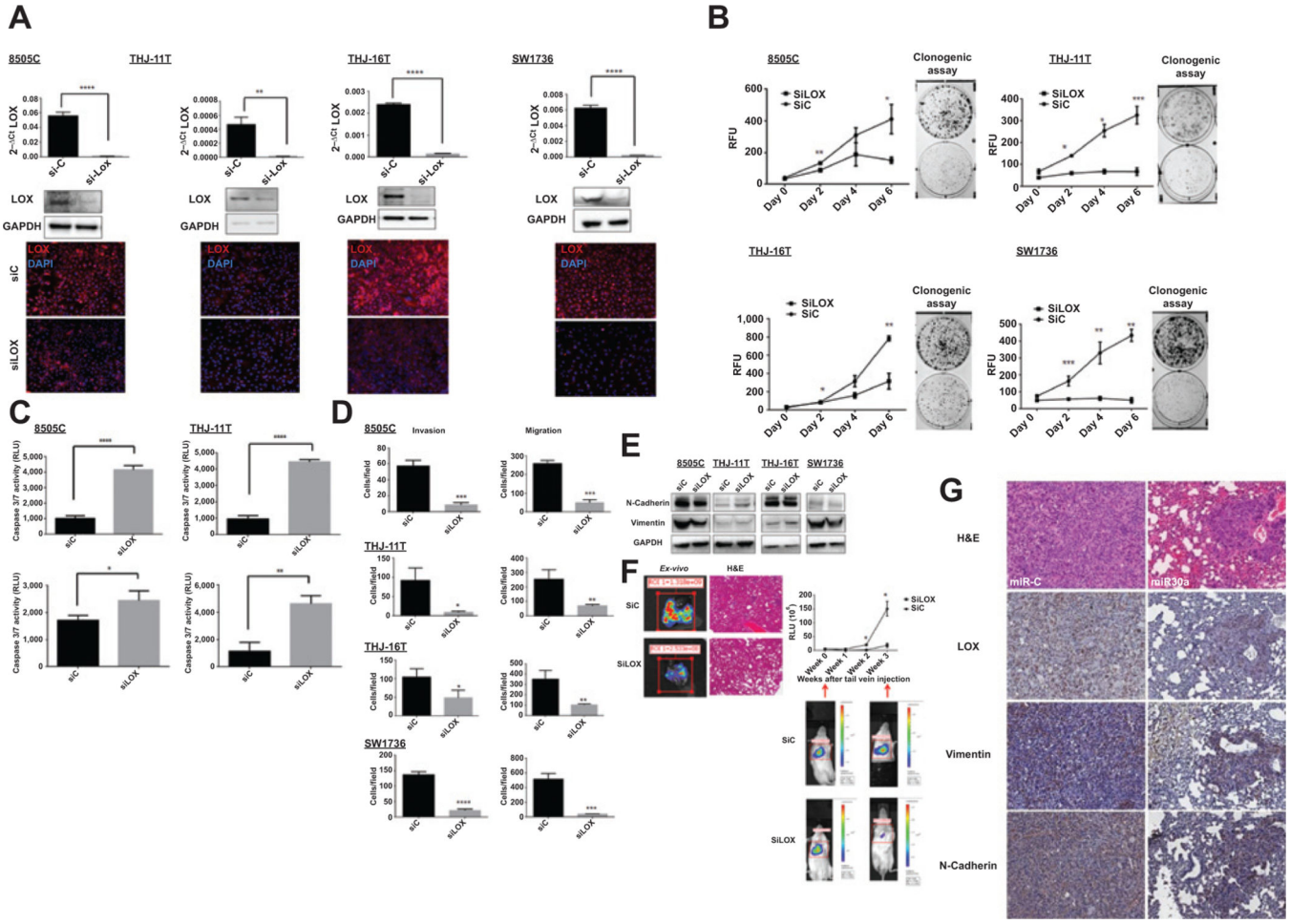

Figure 6.

Effect of *LOX* knockdown on cell invasion, migration, apoptosis, and metastasis. A, *LOX* knockdown, using 28 nmol/L of siRNA, assayed by Western blot analysis, RT-PCR, and immunofluorescent staining. B, *LOX* knockdown reduced cell proliferation and colony formation, as determined by a CyQUANT cell proliferation assay and a clonogenic assay. C, *LOX* knockdown resulted in increased apoptosis. The apoptosis marker, caspase-3/7 activity, was analyzed 72 hours after siRNA transfection. D, *LOX* knockdown decreases cellular migration and invasion. These results are representative of at least three independent experiments. E, immunoblot showing the effect of siLOX on the EMT markers N-cadherin and vimentin 72 hours after transfection. F, *LOX* knockdown reduces metastasis. Representative *ex vivo* images and hematoxylin and eosin (H&E)-stained tissue of *LOX* knockdown samples (left side) and metastasis in mice as measured by luciferase activity (right side) of the 8505c-Luc cells that were injected into the tail veins. The relative luminescence values (RLU) of the three siControl (siC) mice and the three siLOX mice are presented here; *, $P < 0.05$. G, effect of miR30a on LOX and EMT marker expression in our thyroid cancer metastasis mouse model. Lung metastases show lower LOX, vimentin, and N-cadherin expression when miR30a is overexpressed. Representative

immunohistochemical images for LOX, vimentin, and N-cadherin in lung metastases of mice injected with 8505C-Luc cells transfected with miR30a or miR-C. Magnification, ×20.